Investigation of Textile Fabrics Behavior under Compression

Laura NAUJOKAITYTĖ*, Eugenija STRAZDIENĖ

Department of Clothing and Polymer Products Technology, Kaunas University of Technology, Studentų 56, LT-51424 Kaunas, Lithuania

Textile materials during manipulation or in garment formation processes tend to deform and loose their form stability even subjected to low loading. Their deformation behavior is greatly influenced by combination of fabric mechanical properties at low loads. In present paper the new attachment for the tensile tester is presented for the investigation of fabric deformation behavior under compression; the construction and working principle of equipment is discussed. Fabric deformation behavior is investigated compressing two types of specimens: pear loop shaped and plate shape. The obtained load-deformation curves according to their characteristic parts are divided into different zones. Each zone is defined by appropriate parameters. The KES-FB (Kawabata Evaluation System for Fabrics) system is used for the measurements of low stress tensile, shear and bending properties. The relationships between the parameters obtained by new equipment and parameters obtained by KES-FB system as well as with formability parameter are defined. The obtained results revealed that deformation behavior under compression of plate and pear loop shaped fabric specimens is greatly influenced by fabric structure, direction and mechanical properties and it gives the information about fabric formability.

Keywords: compression, bending, buckling, low loads.

INTRODUCTION

Nowadays traditional strength oriented textile testing methods are replaced by methods that are based on determination of the mechanical responses of fabrics subjected to low stresses. These methods are created to simulate the actual fabric loading situation during garment processing and wearing. The obtained data provides useful information in guiding manufacturing and designing processes, predicting formability, tailorability and appearance of fabrics [1 – 3].

Two most widely accepted sets of instruments in the world for the measurement of low stress mechanical properties of fabrics are KES-FB (Kawabata Evaluation System for Fabrics) [4] and FAST (Fabric Assurance by Simple Testing) [5] systems. These two systems are used to investigate the same fabric properties using different measuring principles; they summarize the basic mechanical behavior of fabrics, but do not characterize the visual cloth deformations such as buckling and wrinkling, that are a complex combinations of these parameters [6, 7]. Many new methods are being developed in order to characterize the complex fabric deformations or measure multiple properties through single test [8 – 10]. In these methods different fabric properties are correlated to characteristic peaks or slopes of the load-displacement curves.

Fabric formation into spatial garments or products is also determined by the complex combination of different mechanical properties. During formation textile materials have to deform in their plain so, that they could cover spatial surfaces without forming undesired wrinkles or folds. In early sixties Lindberg [11] defined fabric formability as a product of its bending rigidity and in-plain compressibil-

ity, i. e. its ability to sustain in-plain compression before buckling. Fabric bending behavior since 1930's received a big attention of scientists and is widely investigated by a number of equipment based on simple investigation of fabric deformation under its own weight e. g. cantilever, loop methods [12 – 14] or more sophisticated methods measuring moment – curvature or force – angle relationships [4, 15 – 17]. Less attention is paid to direct measurements of fabric in-plain compression. One of the few attempts of direct measurements of in plain compressibility of fabric plate was done by Dahlberg *et al.* [18, 19] who constructed an apparatus as an attachment to Instron tensile tester, but this method didn't gain a wide acceptance. In most of the fabric formability research works compressibility is substituted by the initial fabric extensibility that was proved by Lindberg [11] to be of the same magnitude as compressibility. This approximation is quite rough thus it can give distorted results.

The objective of the present paper is to provide the method and new attachment for the tensile tester for the investigation of fabric deformation behaviour under compression, the device is also used for registering the buckling force as well as the in-plain compressibility of fabrics at buckling.

MATERIALS AND TEST METHODS

100 % cotton fabric (area density – 138 g/m²; warp density – 24 cm⁻¹; weft density – 23 cm⁻¹) was chosen for the investigation. Four different finishing treatments were applied for the test samples in order to change the bending rigidity parameter. These four groups of fabrics were obtained treating pieces of fabric with PVAc (polyvinyl acetate) stiffener dispersions in water of concentrations differing by 5 g/l (i. e. untreated samples and treated with 5 g/l, 10 g/l and 15 g/l stiffener concentrations). Specimen preparation, pre-conditioning, and testing involved

---

*Corresponding author. Tel.: + 370-37-300205; fax.: +370-37-353989.
E-mail address: *launauj@gmail.com* (L. Naujokaitytė)

standard atmospheric conditions of 20 °C ±2 °C temperature and 65 % ±2 % relative humidity.

A new device designed on the basis of a standard instrument for compression of polymeric materials was created as an attachment for tensile tester. The schematic view of the compression device and the modes of specimen fixing are presented in Figure 1.

a

b   c
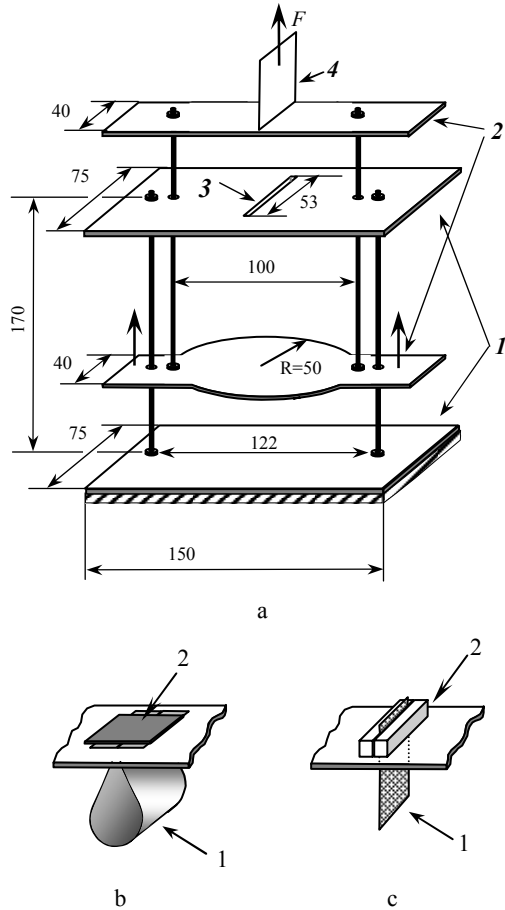
Fig. 1. Scheme of the compression tester: a – construction of the device (linear dimensions are given in mm): 1 – lower stable block; 2 – upper movable compressing block; 3 – aperture for fixing the specimen; 4 – plate for fixing compressing block to the upper clamp of tensile tester; b – fixing scheme of loop shaped specimen in an aperture: 1 – specimen; 2 – fixing plate; c – fixing scheme of plate shape specimen in an aperture: 1 – specimen; 2 – magnetic clamps

The lower stable block 1 (see Fig. 1, a) is rigidly attached to a lower clamp of tensile tester. The specimen is clamped into an aperture 3 of the upper plate of the stable block 1. The movable block 2 is attached via fixing plate 4 to an upper clamp of tensile tester and moves up till its lower plate reaches the specimen and starts compressing it. The load-deformation curve is obtained and the experiment terminates when the predefined deformation is reached. The experiments are performed compressing two types of specimens: loop shaped (Fig. 1, b) and plate shaped (Fig. 1, c).

The deformation behavior of pear loop shaped specimens was investigated in warp, weft and 45° bias directions. Three different dimensions of the specimens were chosen for the investigation: 150 mm × 50 mm,

130 mm × 50 mm and 110 mm × 50 mm. For each fabric and different direction four to six replicate measurements were made, variation coefficient varied between 3 % – 15 %. The distance between the specimen fixing plate and compressing plate was 67 mm. The experiment ends up when the linear compressive deformation $L_{maxkl} = 55$ mm. Speed of the tensile tester is set to 100 mm/min.

The deformation behavior of plate shape specimens was investigated in warp, weft and 45° bias directions. Size of the specimen was 30 mm × 50 mm. For each fabric and different direction six to nine replicate measurements were made, variation coefficient varied between 5 % – 18 %. The distance between the specimen fixing plate and compressing plate was 45 mm. The experiment ends up when the linear compressive deformation of the specimen equals 33 %, i. e. $L_{maxpl} = 25$ mm. Speed of the tensile tester is set to 100 mm/min. The process of experiment must be carefully observed, so that the specimen wouldn't get distorted what can give shell buckling effect with much higher values of buckling force and skewed results.

The KES-FB system [4] was used as a reference data for the determination of the fabric low load mechanical properties such as bending (B – bending rigidity), tensile (LT – linearity of tensile curve, EMT – extension at 490 N/m load) and shear (G – shear modulus, $2HG5$ – shear hysteresis at an angle 5°) properties. In addition to standard KES-FB parameters a non-standard parameter – formability F_{KES} – was also calculated from KES-FB data [20]:

$$F_{KES} = \frac{EMT}{490 \cdot LT} \cdot B \cdot \frac{G}{2HG5},$$ (1)

where: EMT is the extension at 490 N/m load in %, LT is the linearity of tensile curve, B is the bending rigidity in N·m²/m, G is the shear modulus in N/m, $2HG5$ is the shear hysteresis at an angle of 5° in N/m.

Standard samples of 200 mm × 200 mm were tested in warp and weft directions. Four replicate measurements were made for each property. Mechanical properties were measured according to standard KES-FB specifications except for shear test. For the investigation of shear properties maximum shear angle was set to 6 degrees, because the investigated fabrics were prone to buckle before 8 degrees angle (typical for KES-FB) was reached.

RESULTS AND DISCUSSION

The parameters obtained by KES-FB system are presented in Table 1.

In the compression experiment of loop shaped specimens four different stages can be distinguished in the load-deformation curve (Fig. 2, a). The interpretation of stages is done connecting them with particular loop shapes that were captured by a camera during deformation process.

During first stage the lower compressing plate moves up without load till the bottom of the loop is reached, what means the end of stage I (Fig. 2, b). The length of stage I L_0 represents the length of loop from its own weight:

$$L_{k0} = L_{max} - L_0$$ (2)

where: L_{k0} – initial loop length, L_{max} – maximum distance between compressing plates in mm.

Table 1. Parameters obtained by KES-FB system

	Parameter											
	B, N·m²/m		EMT, %		LT		G, N/m·°		$2HG5$, N/m		$F_{KES} \times 10^{-4}$, mm²	
	Fabric direction											
	Warp	Weft	Warp	Weft	Warp	Weft	Warp	Weft	Warp	Weft	Warp	Weft
Co_0	0.054	0.032	4.09	10.96	0.77	0.64	2.19	2.20	4.71	5.32	1.56	1.88
Co_5	0.119	0.060	3.66	9.18	0.83	0.76	2.79	2.82	5.82	6.63	3.45	3.62
Co_10	0.160	0.103	3.17	8.33	0.85	0.82	4.45	4.38	8.67	8.89	4.44	7.07
Co_15	0.240	0.131	2.96	9.91	0.87	0.83	4.59	4.97	9.85	10.23	5.77	8.86
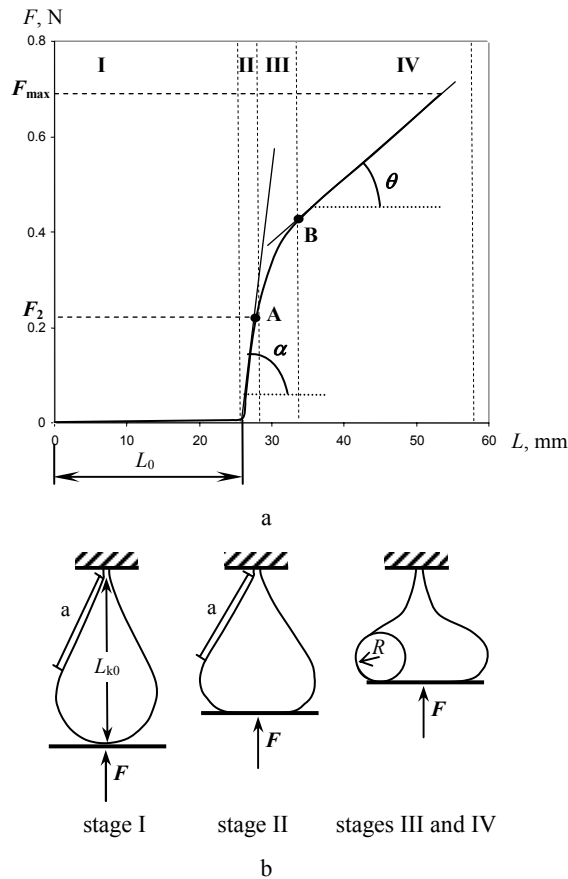
Fig. 2. Deformation of loop shaped specimen: a – load-deformation curve; b – deformation stages and dynamics

Second stage starts with the beginning of deformation process when the lower plate reaches loop bottom and starts compressing it. The contact area between bottom part of the loop and compressing plate is increasing; in the upper part of the loop straight segment "a" is distinguished (Fig. 2, b), its buckling shows the end of stage II (Fig. 2, c). The linear increase of load is observed in load- deformation curve till the point A is reached. The force F_2 is recorded at point A and the inclination of the curve in stage II is described by parameter $tg\alpha$.

In the stage III the inclination of load-deformation curve is observed, its end is marked with the point B, which denotes the beginning of the straight part of the curve and the beginning of stage IV where the predominant deformation is bending; the radius R of the inner contour of the loop is decreasing and the curvature $K = 1/R$ is increasing. The stage IV is described by the maximum

force F_{max} reached at the maximum predefined deformation L_{maxkl} and the inclination of the curve $tg\theta$ (Fig. 2).

Changing the dimensions of the loops changes the length of the characteristic deformation stages as well as characteristic parameters defining these stages. The influence of loop shaped specimens dimensions on the maximum compression force F_{max}, increasing stiffener concentration C is presented in Figure 3. It was found that longer loops (150 mm × 50 mm) due to their lower stability give more scattered results and the F_{max} parameter doesn't show strong linear relationship with increasing stiffener concentration. Decreasing length of the specimens gives lower error of the measurement and the specimens of size 110 mm × 50 mm show the strongest linear relationship between F_{max} and stiffener concentration C ($R^2 = = 0.987 – 0.995$), thus this size of the specimens was chosen for the further investigations.

The values of parameters describing loop compression process for the loop of dimensions 110 mm × 50 mm case are presented in Table 2.

Table 2. Values of parameters describing loop compression

		F_2, N	$tg\alpha$	F_{max}, N	$tg\theta$
		Parameters			
Co_0	Warp	0.015	0.007	0.055	0.0009
	Weft	0.011	0.005	0.043	0.0007
	Bias	0.015	0.004	0.049	0.0008
Co_5	Warp	0.023	0.008	0.067	0.0011
	Weft	0.016	0.005	0.051	0.0009
	Bias	0.023	0.006	0.062	0.0010
Co_10	Warp	0.036	0.011	0.090	0.0015
	Weft	0.024	0.006	0.067	0.0013
	Bias	0.030	0.009	0.077	0.0014
Co_15	Warp	0.042	0.013	0.106	0.0016
	Weft	0.026	0.006	0.071	0.0012
	Bias	0.031	0.009	0.087	0.0015

Loop deformation changes and parameters defining them are related to mechanical and geometrical parameters of the fabrics. From the stage I according to the pear hanging loop method proposed by F. T. Peirce [12] it should be possible to decide about the bending properties of fabrics, but in our case the length of the loops L_{k0} varied with in the limits of 1 mm, thus this parameter is not sensitive in the case of light weight fabrics.
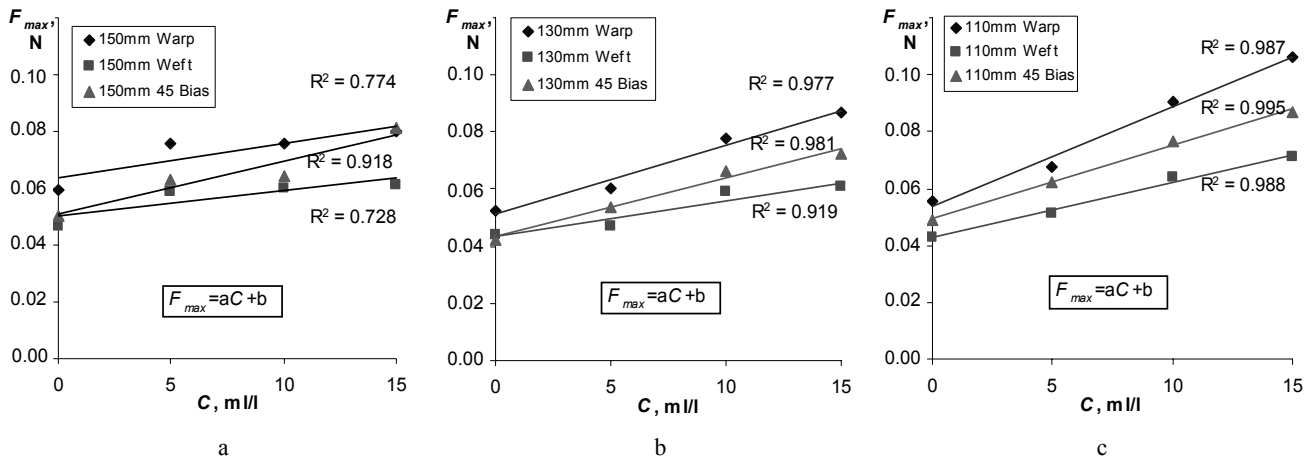
Fig. 3. The influence of specimen size on the maximum loop compression force $F_{\max}$ increasing stiffener concentration C (0 g/l ÷ 15 g/l): a – specimen size 150 mm × 50 mm; b – specimen size 130 mm × 50 mm; c – specimen size 110 mm × 50 mm

During stage II, when the lower compressing plate reaches the loop, it takes all the weight of the loop therefore the correlation between fabric area density w and parameters F_2 and $\mathrm{tg}\,\alpha$ defining second deformation stage is expected. As in stage IV the predominant deformation is bending, the correlation coefficients between bending rigidity B as well as area density w and parameters $F_{\max}$ and $\mathrm{tg}\,\theta$ defining fourth deformation stage was found. Correlation coefficients between fabric mechanical and geometric parameters and parameters obtained by novel compression device are presented in Table 3.

Table 3. Correlation coefficients between fabric area density and bending rigidity with loop compression parameters

Parameters	F_2, N	$\mathrm{tg}\,\alpha$	$F_{\max}$, N	$\mathrm{tg}\,\alpha$
w, g/m²	0.75	0.82	0.89	0.75
B, N·m²/m	–	–	0.98	0.96

Note: "–" – the correlation doesn't exist.

Good correlation coefficients in Table 3 confirm the above made considerations.

During in-plain compression, after reaching certain value of the load, textile fabrics loose their stability and buckling is observed. The load, at which it happens is called buckling force. Before buckling occurs, textile fabrics are deformed in their plain at a certain level, this deformation is called buckling deformation and even though it is very small, but is very important defining fabric formability.

In the plate compression experiment three different stages can be distinguished in the load-deformation curve (Fig. 4, a). The interpretation of stages is done connecting them with particular specimen shapes during deformation process.

During first stage the lower compressing plate moves up without load till the bottom of the specimen is reached, that means the end of stage I (Fig. 4, b). Second stage represents in-plain compression of the specimen till buckling occurs and the sudden increase of the force is observed. The length of the stage II is equal to buckling deformation ε_{kl} and the buckling force F_{kl} is recorded at the end of stage II. After buckling moment, the sudden decrease of force is observed in a load-deformation curve,

followed by a slight increment of force due to the increasing bending moment conditioned by increasing curvature of the specimen (Fig. 4, b).
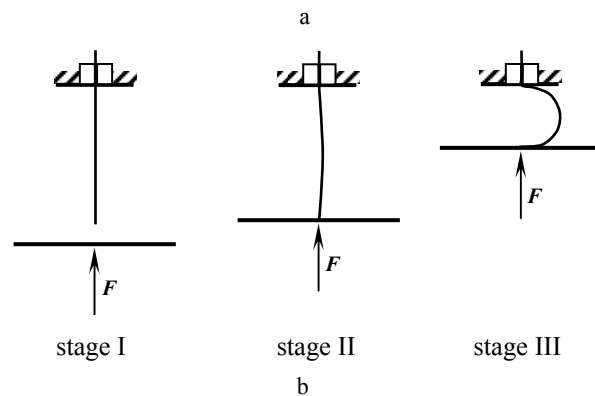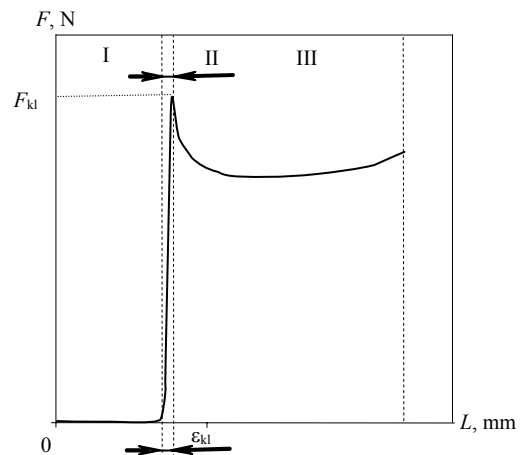
Fig. 4. Deformation of plate shape specimen: a – load-deformation curve; b – deformation stages and dynamics

During in-plain compression in warp or weft direction, the deformations dominate in that yarn system in which direction load is applied, while in perpendicular yarn system deformations are negligibly small, thus the buckling force is mainly dependent on the bending rigidity of yarn system which undergoes deformation. As bending rigidity increases linearly with increasing stiffener concentration, the linear dependence between buckling force and stiffener concentration was found (Fig. 5).

Compressing the fabric in 45° bias direction, deformations consisting of yarn compression and rotation occur in both yarn systems. The changes of the unit cell geometry due to rotation of warp and weft yarns are observed during this deformation. Theoretically critical buckling force should be reached when the shear lock angle is reached, but in reality membrane strains are exceeded much earlier and specimen buckles before shear lock angle is reached. The correlation coefficient between shear rigidity G and buckling force F_{kl} in bias direction was calculated ($r = 0.97$).
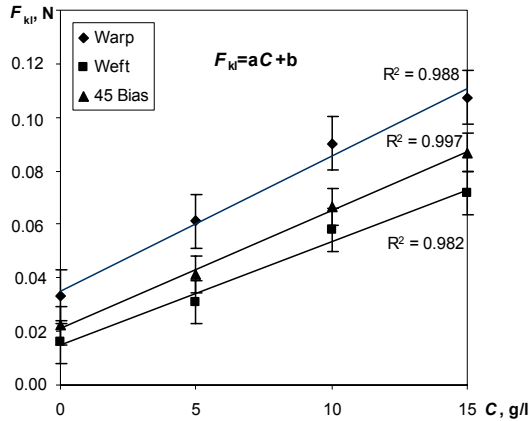

Fig. 5. Dependence of buckling force F_{kl} on stiffener concentration C

In literature [18] it was proved that the plate buckling force varies with the specimen length in approximate agreement with Euler's equation for buckling of bars. In present case the equation of bars rigidly supported at one end is used for the calculation of buckling force:

$$F_{klcalc} = \frac{\pi^2 B}{4l^2}, \qquad (3)$$

where: B is the fabric bending rigidity, l is the specimen length.

From Equation 3 it is seen that keeping constant length of the specimen, the changes of buckling force must be proportional to fabric bending rigidity. A strong linear relationship ($r = 0.98$) between calculated F_{klcalc} and experimental values of buckling force F_{kl} was obtained (Fig. 6).
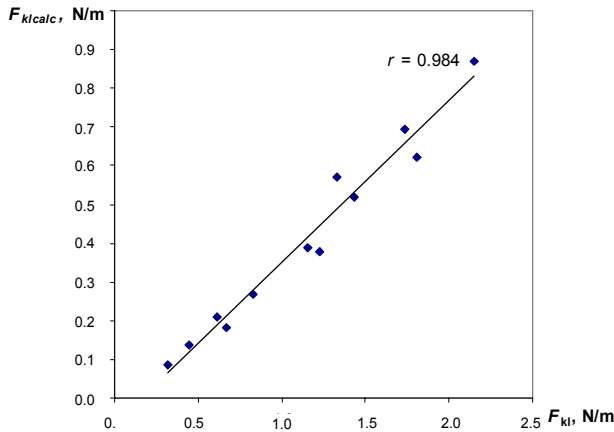

Fig. 6. Correlation between experimental and calculated buckling force

Strong correlations ($r = 0.99$) were obtained between the buckling force F_{kl} and formability parameter F_{KES} (calculated according to eq.1) in both warp and weft directions. This relation shows that the lower is the buckling force of the fabric the lower formability it possesses.

The values of buckling deformation ε_{kl} were determined directly form the obtained load deformation curves (Fig. 7).
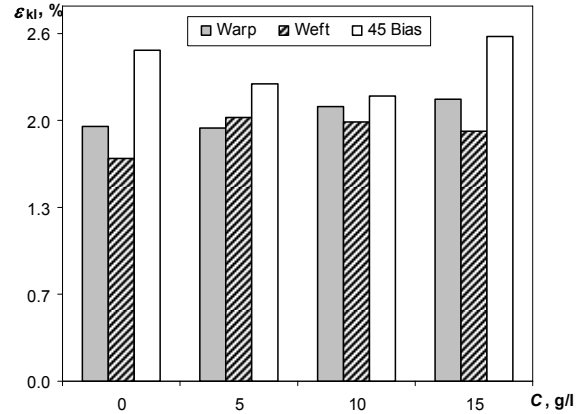

Fig. 7. Dependence of buckling deformation ε_{kl} on stiffener concentration C

These values (Fig. 7) didn't show clear tendencies with increasing stiffener concentration. In warp and weft direction buckling deformation is equal to 1.9 % − 2.1 % and varies within the limits of 0.3 mm, this is determined by the dense structure of the fabric that can't deform within its plain. As expected the buckling deformation in bias direction is a little bit higher (2.1 % − 2.6 %) due to the shear effect.

CONCLUSIONS

In the present paper the new technically simple method for the investigation of deformation behavior of fabrics under compression is presented.

During deformation of loop shaped specimens four main stages can be distinguised in load-deformation curve. The characteristic parameters of each stage depend on specimen dimensions, fabric direction and its mechanical properties. Optimal size of the specimens was set to 110 mm × 50 mm. The parameters defining second stage F_2 and tgα show good correlation with fabric area density, while fourth stage parameters F_{max} and tgθ show strong relationship with bending rigidity B.

In the plate shape specimen deformation experiment the buckling force F_{kl} and buckling deformation ε_{kl} values of the fabrics can be defined. Experimentally obtained buckling force F_{kl} changes in a good agreement with Euler's equation for buckling of bars rigidly supported at one end. Buckling force F_{kl} and buckling deformation ε_{kl} mainly depend on fabric direction and its mechanical properties. Buckling force F_{kl} obtained in principle fabric directions shows good correlation with bending rigidity B and formability F_{KES} parameter of fabrics; in bias direction it shows correlation with the shear modulus G.

REFERENCES

1. **Pan, N., Zeronian, S. H., Ryu, H. S.** An Alternative Approach to the Objective Measurement of Fabrics *Tex. Res. J.* 63 (1) 1993: pp. 33 – 43.

2. **Pavlinic, D. Z., Geršak, J.** Design of The System for Prediction of Fabric Behavior in Garment Manufacturing Processes *Int. J. of Cloth. Sc. and Tech.* 16 (1/2) 2004: pp. 252 – 261.

3. **Leung, M. Y., Lo, T. Y., Dhingra, R. C., Yeung, K. W.** Relationship between Fabric Formability, Bias Extension and Shear Behavior of Outerwear Materials *Res. J. of Text. and App.* 4 (2) 2000: pp. 10 – 23.

4. Kawabata Evaluation System for Fabrics Manual, Kato Tech. Co. Ltd, Kyoto, Japan.

5. Fabric Assurance by Simple Testing, CSIRO Division of Wool Technology. Geelong, Australia, 1997.

6. **Yick, K. L., Cheng, K. P. S., Dhingra, R. C., How, Y. L.** Comparison of Mechanical Properties of Shirting Materials Measured on the KES-F and FAST Instruments *Text. Res. J.* 66 (10) 1996: pp. 622 – 633.

7. **Pascal, V., Thalmann, N. M.** Virtual Clothing: Theory and Practice Berlin, Springer 2000: 283 p. ISBN 3-540-67600-7.

8. **Yazdi, A. A., Amirbayat, J.** Evaluation of the Basic Low Stress Mechanical Properties (Bending, Shearing and Tensile) *Int. J. of Cloth. Sc. and Tech.* 12 (5) 2000: pp. 311 – 325.

9. **Yazdi, A. A., Shahbazi, Z.** Evaluation of the Bending Properties of Viscose/Polyester Woven Fabrics *Fibr. and Text. in East. Eu.* 14 (2(56)) 2006: pp. 50 – 54.

10. **Du, Z., Yu, W.** Analysis of Bending Properties of Worsted Wool Yarns and Fabrics Based on Quasi-three-point Bending *J. of the Text. Inst.* 96 (6) 2005: pp. 389 – 399.

11. **Lindberg, J., Waesterberg, L., Svenson, R.** Wool Fabrics as Garment Construction Materials *J. of the Text. Inst.* 51 (12) 1960: pp. T1475 – T1493.

12. **Peirce, F. T.** The „Handle" of Cloth as a Measurable Quantity *J. of the Text. Inst.* 21 (11) 1930: pp. T377 – T416.

13. **Cassidy, T., Cassidy, C., Cassie, S., Arkison, M.** The Stiffness of Knitted Fabrics: A New Approach to the Measurement of Bending - Part 1: Development *Int. J. of Cloth. Sc. and Tech.* 3 (5) 1991: pp. 14 – 19.

14. **Mete, F., Lloyd, D. W.** Modelling the "CLOACK" Test: an Example of Two-dimensional Elastica Theory *J. of Cloth. Sc. and Tech.* 12 (4) 2000: pp. 255 – 264.

15. **Livsey, R. G., Owen, J. D.** Cloth Stiffness and Hysteresis in Bending *J. of the Text. Inst.* 55 (10) 1964: pp. T516 – T530.

16. **Abbott, G. M., Grosberg, P.** Measurement of Fabric Stiffness and Hysteresis in Bending *Text. Res. J.* 36 (10) 1966: pp. 928 – 930.

17. **Ozcelik, G., Fridrichova, L., Bajzik, V.** The Comparison of Two Different bending Rigidity Testers *4th CEC Conference Proceedings* 2005: pp. 1 – 6 (CD edition).

18. **Dahlberg, B.** Mechanical Properties of Textile Fabrics Part II: Buckling *Text. Res. J.* 31 (2) 1961: pp. 94 – 99.

19. **Lindberg, J., Behre, B., Dahlberg, B.** Part III: Shearing and Buckling of Various Commercial Fabrics *Text. Res. J.* 31 (2) 1961: pp. 99 – 122.

20. **Harlock, S. C.** Fabric Objective Measurement: 4, Production Control in Apparel Manufacture *Text. Asia* 20 (7) 1989: pp. 89 – 98.